PHYSICAL REVIEW B VOLUME 43, NUMBER 10 1 APRIL 1991

Surface-impedance measurements of superconducting NbN films

D.E. Oates and Alfredo C. Anderson
Lincoln Laboratory, Massachusetts Institute of Technology, Lexington, Massachusetts 02173

C.C. Chin
Department of Physics, Massachusetts Institute of Technology, Cambridge, Massachusetts 02139 and Rome Air Development Center, U.S. Air Force, Hanscom Air Force Base, Massachusetts 01731

J.S. Derov
Rome Air Development Center, U.S. Air Force, Hanscom Air Force Base, Massachusetts 01731

G. Dresselhaus
Francis Bitter National Magnet Laboratory, Massachusetts Institute of Technology, Cambridge, Massachusetts 02139

M.S. Dresselhaus
Department of Electrical Engineering and Computer Science and Department of Physics, Massachusetts Institute of Technology, Cambridge, Massachusetts 02139
(Received 7 November 1990; revised manuscript received 12 February 1991)

The temperature and frequency dependences of the surface impedance of NbN thin films have been measured from 4.2 to 13 K and from 0.5 to 10 GHz using a stripline resonator. At 4.2 K resonant-cavity measurements of surface resistance were made at 35 and at 56 GHz. From surface-reactance measurements using both cavity and stripline techniques, we obtain the penetration depth extrapolated to 0 K, $\lambda(0) = 3700$ Å. For the stripline, the film thickness was approximately 8000 Å, which is about two times the measured penetration depth. The weak-coupling Mattis-Bardeen theory was used to fit the temperature dependence of the surface resistance. Based on the quality of the weak-coupling fit to the data, we conclude that the strong-coupling effect is not important in the local and dirty limits. We discuss the correction due to the finite film thickness of the stripline measurements of the surface resistance.

I. INTRODUCTION

The discovery of the high-T_c copper oxide superconductors has heightened interest in many passive microwave device applications, including resonators, filters, delay lines, and other signal processing components that can operate at temperatures as high as that of liquid nitrogen. However, the surface resistance at 4.2 K of high-T_c copper-oxide thin films is still higher than that of Nb, despite the recent improvements in the deposition techniques. The deposition of NbN thin films of very low surface resistance (comparable with Nb) and of relatively high-T_c (14–17 K) is still of great interest for application to microwave devices. Also, measurements of the temperature and frequency dependence of the surface impedance[1] provide information on the coupling mechanism of the superconducting electron pairs, which is of interest for both the physics and materials science of NbN.

NbN is also of interest for the further development and understanding of the cuprate superconductors, because it is a granular material as are the cuprates, yet with its mechanism of superconductivity better understood. Furthermore, until the cuprate superconductors are proven to be practical materials, NbN is perhaps the best candidate for applications at higher temperatures than would be possible for niobium. For example, the microwave cavities for superconducting particle accelerators now use Nb below 4.2 K, but a viable NbN technology that produces material of low microwave losses might well be of considerable interest for this application.

The temperature and frequency dependences of the surface resistance of NbN were measured using a stripline resonator from 4.2 to 13 K and from 0.6 to 10 GHz. At 4.2 K resonant cavity measurements were made at 35 and 56 GHz. The penetration depth $\lambda(T)$ was measured in a Cu cavity at 35 GHz and in the stripline at 0.58 GHz, and the data were extrapolated to $T \rightarrow 0$. The agreement between the stripline and cavity measurements of R_s and $\lambda(0)$ is good, although the thickness of the center conductor of the stripline is comparable with the penetration depth. This is the first confirmation that stripline and cavity measurements of R_s and $\lambda(0)$ agree. Such agreement is important because both methods are being used to characterize high-T_c superconducting films. The

TABLE I. Superconducting parameters of NbN as measured by various authors.

Parameter	Value	Technique	Best fit[a]
$2\Delta/kT_c$	4.31[b], 4.21[c]	Tunneling	4.31
	4.75[d]	Microwave	
$\lambda(0)$ (Å)	3750[e]	Microwave	3700
	3700[d]	Microwave	
ξ_0 (Å)	350[f]	Specific heat	350
ℓ (Å)	3.8[g], 6.6[f]	Resistivity	3.8

[a]From the analysis in this paper.
[b]Reference 7.
[c]Reference 8.
[d]The BCS model fit to R_s measurements at 35 GHz.
[e]From cavity measurements at 10 GHz (Ref. 9).
[f]From normal-state resistivity of polycrystalline thin film (Ref 10).
[g]From normal-state resistivity of thin single crystal (Ref. 11).

NbN stripline devices can be made either in the thick or the thin limit [compared to $\lambda(0)$] and thus allow us to examine the finite film thickness effect experimentally.

Mattis and Bardeen[2] have calculated the surface impedance based on the isotropic weak-coupling BCS theory for the extreme anomalous limit $\lambda \ll \xi_0$, where ξ_0 is the BCS coherence length for a superconductor. The extreme-anomalous-limit criterion of the Mattis-Bardeen theory[2] was generalized by Turneaure[3] and independently by Halbritter[4] to include the effect of the London penetration depth λ_L, ξ_0, and the electron mean free path ℓ. Nam[5,6] extended the Mattis-Bardeen theory to the case of strong-coupling superconductors. However, to apply Nam's theory requires knowledge of the details of the electron-phonon spectrum $\alpha^2F(\omega)$, which was measured by tunneling,[7,8] and there is some discrepancy in the reported values of $\alpha^2F(\omega)$. The pertinent superconducting parameters for NbN are given in Table I, showing that NbN is in the strong-coupling limit and also in the local ($\lambda \gg \xi_0$) and dirty ($\ell \ll \xi_0$) limits. At this time the Nam theory has not been put into a form that makes it readily applicable to a numerical calculation of the surface resistance of a strong-coupling superconductor.

We have successfully applied the weak-coupling surface impedance theory of Turneaure[3] and Halbritter[4] to fit the experimental data of the strong-coupling superconductor NbN, which is in the local and dirty limits. The experimental validity of the generalized Mattis-Bardeen theory implies that $\alpha^2F(\omega)$ is not an important parameter in describing the temperature dependence of the surface resistance of NbN.

II. EXPERIMENTAL

A. Sample preparation

The NbN films used in this study were deposited on a sapphire substrate by dc magnetron sputtering of a pure Nb target in an argon and nitrogen sputtering gas using the parameters shown in Table II. The preparation method has been described in detail previously.[12] Although the samples were not heated intentionally, the substrate temperature during deposition rose to ~280 °C. The superconducting transition temperature (determined as the resistivity midpoint by a four-point method) for samples deposited under the same conditions is 15.8 K, which is slightly higher than the microwave measurements. The T_c measured by the microwave reactance measurements described below is 15.3 K. A small difference between the resistive and reactive measurements of T_c is not unusual. The resulting films are stoichiometric NbN (within 5%) as determined by Auger electron spectroscopy and Rutherford backscattering. A small amount of oxygen and carbon (less than 1%) is also present in the films. X-ray diffraction shows that the films are highly textured with their (111) axes preferentially oriented perpendicular to the substrate. The average crystal size was measured on a transmission electron microscope planar view to be approximately 50 Å. The critical current density J_c at 4 K was measured by dc transport to be 2.5×10^6 A/cm^2. A film thickness of about 8000 Å was used in the stripline, and film thicknesses of both ~1.5 and 3.0 μm were used for the samples measured in the cavities. The characteristics of the films reported in this paper are summarized in Table III.

TABLE II. Magnetron sputtering parameters of NbN.

Argon pressure	10 mT
Nitrogen flow	2.1 SCCM[a]
Substrate to target distance	4.8 cm
DC power	290 W
Deposition rate	0.29 nm/s

[a]Cubic cm per minute at standard temperature and pressure.

B. Stripline resonator measurements of R_s and λ

1. Measurements of R_s

Measurements of R_s as a function of frequency from 0.6 to 20 GHz and as a function of temperature over the range 4.2 to ~13 K have been made with a transmission-line resonator using a stripline geometry.[13,14] A stripline as shown in Fig. 1(a) is defined as having a center conductor, an upper and lower ground plane, and a symmetric dielectric. The resonator, seen most clearly in the top view of Fig. 1(b), consists of an isolated length of transmission line one-half-wavelength long at the fundamental frequency. Overtone resonances occur at all multiples of the fundamental frequency. The resonator is capacitively coupled to the external circuit by gaps at the two ends of the stripline [see Fig. 1(b)]. In our case the length of line was chosen to yield a fundamental frequency of approximately 0.6 GHz and the linewidth and thickness were 150 and 0.8 μm, respectively. The resonator is fabricated on a $25\times12.5\times0.5$-mm^3 sapphire dielectric ($\epsilon = 10$) to give about 50 Ω for the transmission line impedance. The stripline was fabricated using standard photolithography

TABLE III. Characteristics of sample NbN films.

Sample	Thickness (μm)	T_c (K)	Method	R_{res} ($\Omega/\Box$)[a]	$\lambda(0)$ (Å)
1	0.8	15.3	Stripline[b]	1×10^{-7}	3850
2	1.5	15.3	Nb cavity[c]	1.5×10^{-3}	
2	1.5	15.3	Cu cavity[d]		3700
3	1.5	15.6	Cu cavity[d]		3400
4	3.0	15.3	Cu cavity[d]		3700

[a] Residual R_s (see Sec. III C).
[b] 0.5 GHz.
[c] 56 GHz.
[d] 35 GHz.

and the film was etched in a CF_4 plasma-etching system. The stripline together with two ground planes is mounted in a gold plated copper package with rf connectors on it.

The resonator Q can be determined by finding the 3-dB points of the curve of transmitted power versus frequency as measured in a network analyzer. We have measured the Q of the fundamental and overtone resonances from 0.6 to 10 GHz from 4.2 to 13 K. In addition, measurements from 10 to 20 GHz were made at 4.2 K. The surface resistance R_s is extracted from the Q measurements by the method described below.

The ultimate sensitivity of the R_s measurements using the stripline method is better than 10^{-7} Ω as has been demonstrated with niobium films at 4.2 K.[13] This resonator structure concentrates the losses in the center conductor because the narrow ($\sim$150-μm) line results in a much higher current density in the center conductor than in the ground plane. A major advantage of the stripline geometry is the low radiation losses that result from the presence of upper and lower ground planes. The ground planes thus confine the field almost completely so that stray coupling to other conductors and extra electromagnetic energy losses thus caused are virtually eliminated. Striplines produce the highest Q of any of the transmission-line structures. The stripline method also has the advantage that measuring the frequency dependence of R_s is relatively simple, in that many harmonics are measured with the same stripline device. By contrast,

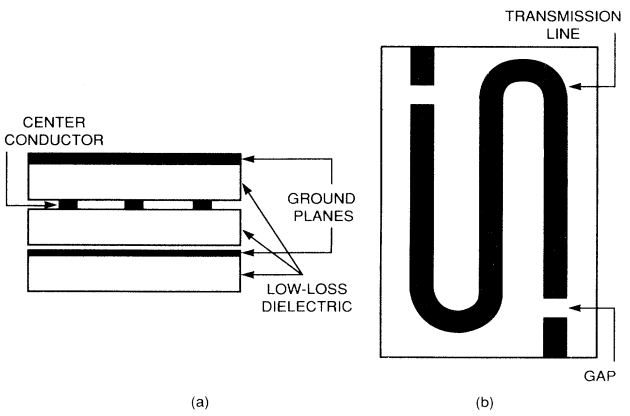

FIG. 1. Schematic diagram of the stripline resonator showing (a) the cross section and (b) a top view.

in the most widely used configurations of microwave cavity measurements the cavity is fixed in frequency, and a separate cavity is needed for each frequency.

The following discussion outlines the method by which we calculate R_s from the measured stripline resonator Q. The dielectric losses in the sapphire substrate are neglected because of the very small measured loss tangent.[15] We properly adjust the resonator coupling by varying the size of the coupling gap [see Fig. 1(b)] to be in the weak-coupling limit. When the insertion loss at resonance is 20 dB or greater, the weak-coupling condition is obtained. Then $Q_L \simeq Q_C$, where Q_L is the measured (loaded) Q and Q_C is the material Q. The unloaded Q_C is related to α, the attenuation constant for the line, by

$$Q_C = \frac{\pi}{\alpha \lambda_{em}}, \tag{1}$$

where α is in Np/m and λ_{em} is the wavelength of the microwaves in the dielectric. When the magnetic penetration depth is small compared to the thickness of the conductors, α can be related to the surface resistance and current distribution by

$$\alpha = R_s \frac{\int_0^w K^2(x)dx}{2Z_0 I_0^2}, \tag{2}$$

where x is the lateral dimension of the line of width w, $K(x)$ is the surface current (current per unit width) in the conductors, Z_0 is the characteristic impedance of the line, and I_0 is the total current in the line. The surface current $K(x)$ is given by

$$K(x) = \int_0^t J(x,y)\, dy, \tag{3}$$

where t is the thickness of the film, y is the direction perpendicular to the film and $J(x,y)$ is the current density. It is important to note that in Eq. (2) one only needs to know the integral of the square of the current distribution in order to calculate the surface resistance from the measured Q. The detailed current distribution need not be known exactly provided the local currents do not exceed the superconducting critical current.

To calculate the integral of the square of the current distribution, we follow an incremental inductance method first suggested by Wheeler[16] and arrive at the following expression:

$$\alpha = \frac{\sqrt{\epsilon_r}}{Z_0}\sqrt{\frac{\epsilon_0}{\mu_0}}\left(\frac{\partial Z_0}{\partial h} - \frac{\partial Z_0}{\partial w} - \frac{\partial Z_0}{\partial t}\right)R_s, \tag{4}$$

where ϵ_r is the dielectric constant of the dielectric, h is the distance between the center of the center conductor and each of the ground planes, w is the width, and t is the thickness of the center conductor. Equation (4) can be evaluated using one of the many approximate functional forms for Z_0 that appear in the literature. We used the expression given by Wheeler[17] to obtain, for $h = 410$ μm, $w = 150$ μm, and $t = 0.8$ μm, the value $\alpha = 5.55 \times 10^{-2} R_s$ m^{-1}, where R_s is in ohms. By using Eq. (1) the surface resistance is

$$R_s = \left(\frac{f_0}{Q_C}\right)\Gamma_G, \tag{5}$$

where f_0 is the resonant frequency and Γ_G is a geometrical factor for the resonator, which for this particular stripline geometry is 0.55 Ω/GHz. Equation (5) can be used to relate Q_C to R_s for the particular geometry used here.

Equation (5) is valid only when the magnetic penetration depth λ of the superconductor is small compared to the thickness t of the films. In that limit, Eq. (5) yields the surface resistance R_s of a semi-infinite slab of material as it is normally defined.[18] When, however, the penetration depth becomes comparable to the film thickness, Eq. (5) yields an effective surface resistance in the stripline which is larger than that of the semi-infinite slab because of the increased current density. In order to correct for the finite t/λ, one needs to know the detailed current distribution. To a sufficient approximation, we can correct the measured surface resistance with a $\coth(t/2\lambda)$ factor[19,20]

$$R_s = \frac{0.55(f_0/Q_C)}{\coth(t/2\lambda)}, \tag{6}$$

as is discussed in the Appendix [see Eq. (A6)]. This correction is exact for the case of a uniform current distribution. Even though the current distribution is not uniform for our measurements, this correction factor is sufficiently accurate since the corrections are small. More exact calculations[19] have shown that in the temperature range of these experiments, the corrected R_s given by Eq. (6) is accurate to within 10%. To apply the correction for small t/λ to our data, one must know λ accurately.

2. Measurements of the penetration depth λ

We have determined λ using the stripline resonator by measuring the resonance frequency versus T. In the case of the stripline resonator the resonance frequency is proportional to $1/\sqrt{L}$, where L is the inductance per unit length of the stripline. L in turn is a function of λ and of the specific geometry of the stripline. The inductance $L(\lambda)$ has recently been calculated[19] for the geometry used in these measurements. It should be emphasized that because of the nonuniform distribution of currents in the center conductor of the stripline, the usual expression for L derived for the uniform currents[20] of a parallel plate transmission line is not applicable.

C. Cavity measurements of R_s and X_s

1. Measurements of R_s

Measurements of R_s at 35 and 56 GHz were made using a one-port cylindrical Nb cavity in which one endplate was replaced by the NbN film to be measured. The loaded Q_L was determined[21,22] by measuring the resonant frequency f_0, the magnitude of the reflection coefficient at resonance $[|S_{11}(f_0)|]$, and the width of the resonance taken at half maximum $\Delta f_{1/2}$, where

$$|S_{11}(f_0 + \Delta f_{1/2}/2)|^2 = \frac{1 + |S_{11}(f_0)|^2}{2}. \tag{7}$$

This gives the loaded Q_L of

$$Q_L = \frac{f_0}{\Delta f_{1/2}}. \tag{8}$$

The unloaded Q_C can be determined from this measurement if lossless coupling is assumed. Then for the undercoupled case Q_L is related to Q_C by

$$\frac{Q_C}{Q_L} = \frac{2}{1 + |S_{11}(f_0)|}. \tag{9}$$

R_s is then given by Eq. (5) with the geometrical factor Γ_G for the niobium cavities being 10.8664 and 6.7216 Ω/GHz for the 35- and 56-GHz cavities, respectively.[23]

The cavity was operated in the TE_{011} mode, and the degeneracy between the TE_{011} and the TM_{111} modes[18,24] was removed by cutting a chamfer into the cylinder at the endwall of the cavity. The cavity was placed inside a tube that was backfilled with He gas to prevent any oxygen or water vapor from entering the resonant cavity. The Q_C of the all-niobium cavity was measured to determine the surface resistance of the pure niobium. One Nb endwall of the cavity was then replaced by the NbN film, and film, and the cavity Q_C was remeasured to determine the surface resistance of the NbN film using the expression

$$R_s(\mathrm{NbN}) = f_0\Gamma_G\left(\frac{1}{Q_C(\mathrm{NbN})} - \frac{1}{Q_C(\mathrm{Nb})}\right) + R_s(\mathrm{Nb}), \tag{10}$$

where R_s(Nb) and R_s(NbN) are the surface resistances of niobium and of the test film, respectively, Q_C(Nb) is the Q_C of the all-niobium cavity, Q_C(NbN) is the Q_C with the Nb endwall replaced by the NbN film under test and Γ_G is the geometrical factor for the endface alone and is 60.6 and 48.3 Ω/GHz for the 35- and 56.6-GHz cavities, respectively.

2. Measurement of λ

To determine λ using the resonant cavity, the temperature dependence of the reactance was measured using a 35-GHz two-port cylindrical copper cavity in the TE_{011} mode with the same basic structure as the Nb cavity described above. One endface of the cavity was replaced with the film to be tested. The surface reactance X_s was determined by measuring the shift of the resonance frequency as a function of the temperature and by using the expression[23,25]

$$\frac{f(T)-f(0)}{f(0)} = -\Gamma_C \, \Delta X_s, \tag{11}$$

where T is the temperature, $f(T)$ is the resonance frequency, Γ_C is a geometrical factor of the cavity (given by 187.33 Ω/GHz as calculated from the Slater equation[23]), and ΔX_s is the change of the surface reactance with respect to 0 K. ΔX_s is given by

$$\Delta X_s = \mu_0 \omega \, \Delta\lambda, \tag{12}$$

so measurement of $\Delta\lambda$, the change of penetration depth with respect to 0 K, follows directly from measurement of the shift in the resonant frequency of the resonator.

III. RESULTS

The surface impedance for superconducting NbN films was measured by both the cavity and stripline techniques. In both cases, the Q and the resonant frequency of the resonator were measured as a function of temperature and frequency. From these results it is possible to deduce the surface impedance for a plane wave incident on a semi-infinite superconductor, which is the theoretical quantity calculated. The reduction of the data for cavity measurements is relatively straightforward,[25] whereas the stripline data require corrections associated with the finite thickness of the superconducting films in comparison with $\lambda(T)$. These points are addressed in this section.

A. Determination of penetration depth

An accurate determination of the penetration depth is important for the characterization of the NbN films. An independent measurement of λ is needed for the determination of R_s from the measurements of Q in the stripline resonator experiments; as discussed above, the thickness of the film used in the stripline resonator (8000 Å) is comparable to the expected λ. The penetration depth also is a necessary parameter for fitting the measured R_s data to calculated values. Further, an independent measurement of the penetration depth allows a more accurate determination of other important superconducting parameters such as the energy gap and coherence length.

1. Cavity

Figure 2(a) shows the measurement of $X_s(T) - X_s(0)$ versus temperature for the NbN film of thickness 3 μm (sample 4 in Table III). The open squares are the measured data and the solid line is a least-squares fit to the data using the weak-coupling (full) Mattis-Bardeen theory, and the computer code of Turneaure[3,4] for the numerical computations. The parameters used in the computation are the transition temperature $T_c = 15.3$ K determined by observing the discontinuity in the slope of $X_s(T)$ at the normal-superconducting transition, the gap at zero temperature $2\Delta(0)/(kT_c) = 4.31$ (obtained from tunneling experiments[7]), the coherence length[10] $\xi_0 = 350$ Å (see Table I), and the Fermi velocity v_F deduced from[26]

$$\xi_0 = \frac{\hbar}{\pi} \frac{v_F}{\Delta(0)}. \tag{13}$$

We also used the normal-state resistance, measured just above T_c to be 144 $\mu\Omega$ cm, and the electron mean free path ℓ that was deduced from the free-electron expression[27]

$$\ell = 9 \times 10^{11} \hbar (3\pi^2)^{1/3} [e^2 \rho (n^{2/3} S/S_F)]^{-1} = 3.8 \text{ Å}, \tag{14}$$

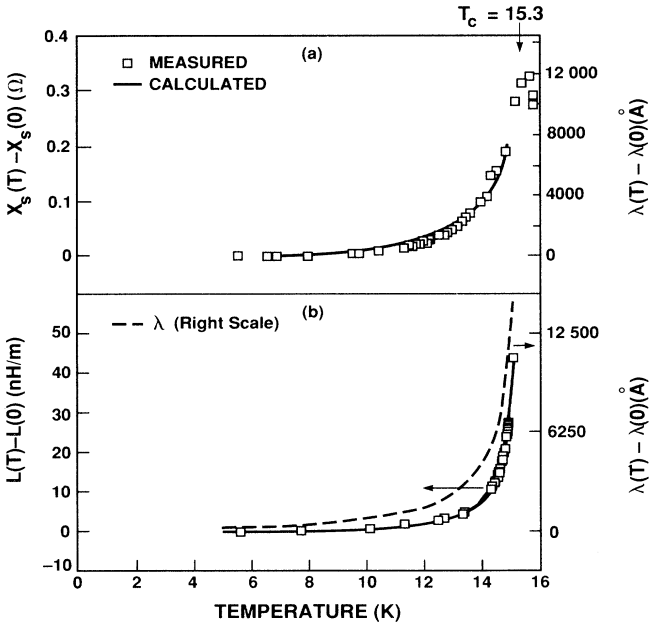

FIG. 2. (a) Temperature dependence of X_s as measured in a 35.6-GHz copper cavity. The solid line is a least-squares best fit to the data points (open squares) calculated using the Mattis-Bardeen model with $\lambda(0) = 3700$ Å and $T_c = 15.3$ K. (b) Change in inductance per unit length $L(T)$ as a function of temperature in the stripline resonator. The solid line is a least-squares best fit to the inductance measurements and is calculated using the Mattis-Bardeen model with $\lambda(0) = 3850$ Å and $T_c = 15.3$ K. The dashed line in (b) is the computed $\lambda(T)$ as deduced from the inductance measurements on the stripline (solid line) and is given by the scale on the right side.

where the resistivity ρ is measured in Ω cm, the free carrier concentration is $n \approx 2.39\times10^{23}/\text{cm}^3$, and $S/S_F = 0.6$ (for most metals)[10] is the ratio of the area of the Fermi surface to that of a free-electron Fermi surface for that carrier density. The penetration depth $\lambda(0)$ was used as an adjustable parameter in fitting the experimental data to minimize the squared differences between measured and calculated values. The best fit is obtained with $\lambda(0) = 3700 \pm 300$ Å. From $\lambda(0)$ we can obtain the London penetration depth[26] $\lambda_L(0)$ from the expression $\lambda(0) = \lambda_L(0)\sqrt{\xi_0/\ell}$, which gives 386 ± 42 Å.

Two other samples were measured in the copper cavity and the results are summarized in Table III.

2. Stripline

Figure 2(b) shows the change in the measured inductance of the stripline versus T using the same films that were used in the Q measurements to determine R_s. The points are the measured data and the solid line is a least-squares fit to the inductance data using the Mattis-Bardeen theory with the same parameters that were used to fit the cavity reactance data and with $\lambda(0)$ as a free parameter. The best fit is obtained with $\lambda(0) = 3850$ Å.

The agreement between the cavity measurements and the stripline measurements of λ is good. Determination of λ in this manner can only be considered accurate to approximately 20% and is model dependent. For example, the two-fluid model gives λ values about 10% larger than the Mattis-Bardeen theory. The value of λ is also highly sensitive to the value of T_c chosen. In the case of the stripline measurements, for instance, a shift of 0.1 K in T_c can change $\lambda(0)$ by 10%. Taking into account these contingencies, we infer a value of $\lambda(0) = 3700 \pm 300$ Å. This value is used in the analysis of the experiments presented in the following section.

B. Measurements of R_s

1. Cavity

The results of the cavity measurements of R_s at 35 and 56 GHz are shown in Fig. 3, which compares the cavity and stripline data. The solid line in the figure is a least-squares best fit to the stripline data assuming the functional dependence $R_s \propto f^2$. The extrapolation of the fit to the stripline data agrees, within experimental error, with the cavity measurements. The R_s measured in the cavity was not corrected for the effects of finite film thickness because $t/\lambda \approx 10$ and the correction is less than 1%.

2. Stripline

Figure 4 shows R_s versus frequency for the stripline for several but not all of the temperatures measured. The values of R_s shown in Fig. 4 are uncorrected for the finite film thickness. The points correspond to the overtones of

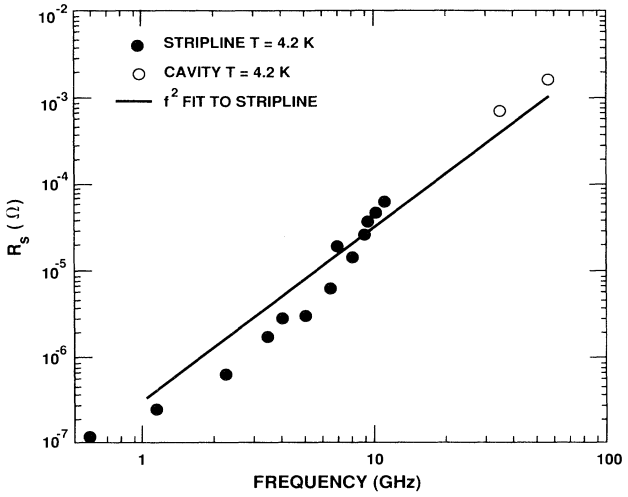

FIG. 3. Frequency dependence of R_s for a NbN film at 4.2 K. The low-frequency points are stripline measurements corrected for the effects of finite film thickness. The 35- and 56-GHz values are measurements in a superconducting Nb cavity. The solid line is a least-squares fit of the stripline data to a f^2 dependence.

the resonator. Lines are drawn to connect points at each temperature. As can be seen, several overtones have R_s values that apparently do not vary with temperature at low temperatures. The Q of these overtone resonances is limited not by the superconducting NbN but by low-Q modes of the resonator package. The modes that show little dependence of R_s on temperature were excluded from the fitting process described below. At the highest temperature plotted in Fig. 4 (13.1 K) the losses in the NbN are sufficiently large that surface resistance is controlled by the NbN and the curve is monotonic.

In Fig. 5 the values of R_s measured in the stripline and corrected for finite t/λ (using $\lambda(0) = 3700$ Å) are shown versus temperature with frequency as a parameter (Fig. 5 includes all temperatures measured). But as noted above, overtone modes for which the apparent R_s was independent of temperature have been excluded from Fig. 5. The solid lines correspond to the theory discussed in the following section.

C. Comparison of data with theory

The data were compared with values computed from the Mattis-Bardeen theory using the numerical program of Turneaure.[3] The parameters used to calculate the surface resistance $R_s(T)$ were the same as those to calculate the temperature dependence of $\lambda(T)$, in order to fit the reactance data in Sec. III A. Before comparing the data with the theory, however, the effects of residual surface resistance must be considered. The experimentally measured $R_s(\omega, T)$ can be written as

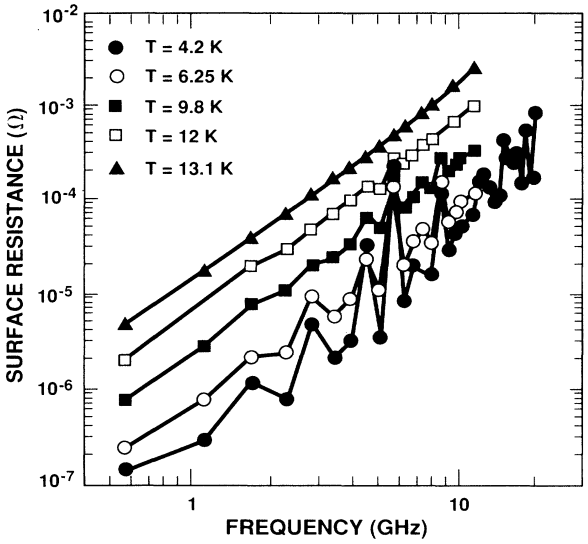

FIG. 4. Frequency dependence of R_s measured in the stripline resonator at various temperatures. The data are uncorrected for finite film thickness. The lines are drawn connecting the points to aid the eye.

$$R_s(\omega,T) = R_{\rm th}(\omega,T) + R_{\rm res}(\omega), \tag{15}$$

where $R_{\rm res}(\omega)$ is the temperature-independent residual surface resistance at angular frequency ω, and $R_{\rm th}(\omega,T)$ is the corresponding temperature-dependent surface resistance calculated from the Mattis-Bardeen model in the superconducting phase. The residual surface resistance

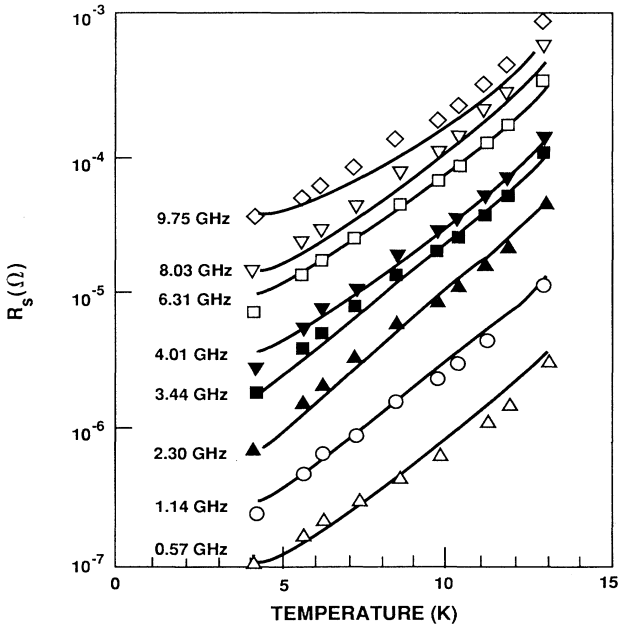

FIG. 5. Temperature dependence of stripline R_s data for various frequencies. The solid lines are calculated from the Mattis-Bardeen theory with parameters given in Table I.

$R_{\rm res}$ comes from surface defects or from carrier scattering at the grain boundaries, inclusions of normal material, and other scattering mechanisms. $R_{\rm res}$ is found in all measurements of R_s in superconductors. It is the quantity $R_{\rm th}(\omega,T)$ that is compared with theory.

Figure 5 shows the corrected stripline surface-resistance data (using $\lambda = 3700$ Å), with the solid lines calculated from the Mattis-Bardeen theory with $2\Delta(0)/kT_c = 4.31$, and $\lambda(0) = 3700$ Å. We have added $R_{\rm res}(\omega)$ to each theoretical curve to account for residual resistance effects, where $R_{\rm res}(\omega)$ was determined by using the measured R_s at 4.2 K.

The measured R_s can be used to independently measure the energy gap by fitting the BCS model expression to the data for $T \leq 9$ K. In the BCS model[20]

$$R_{\rm th} \propto \frac{1}{T}\exp\left(\frac{-\Delta(T)}{kT}\right). \tag{16}$$

The fit to our corrected stripline R_s data shown in Fig. 5 gives $2\Delta(0)/kT_c = 4.75 \pm 0.25$, which is to be compared with the value of 4.31 obtained from the tunneling experiments. Halbritter[28] pointed out that the smaller energy gap determined by tunneling may be caused by a degraded surface layer resulting from oxide formation.[29] Since, however, the difference between the value determined by tunneling and that determined by stripline measurements is small and since the overall fit is not affected much because $R_{\rm th}$ is more sensitive to λ than to Δ, we have used $2\Delta(0)/kT_c = 4.31$ in calculating $R_{\rm th}$ for the comparisons with data shown in Fig. 5.

As seen in Fig. 5, the fit is reasonably good over the entire temperature and frequency range of measurement. Thus, both $\lambda(T)$ and $R_s(\omega,T)$ are fitted very well by the set of parameters chosen (see Table I) and by the Mattis-Bardeen theory.

IV. DISCUSSION

Nam has already deduced the dirty and local limit of his generalized strong-coupling theory.[6] In Nam's paper, the response function $\mathcal{K}(q,\omega)$ is defined by the constitutive equation

$$J(q,\omega) = \frac{-1}{4\pi}\mathcal{K}(q,\omega)A(q,\omega), \tag{17}$$

where $J(q,\omega)$ is the Fourier transform of the current density and $A(q,\omega)$ is the vector potential. The response function is expressed in the local limit [$\mathcal{K}(q,\omega)$ independent of q] and the dirty limit ($\ell \ll \xi_0$) by

$$\mathcal{K}(q,\omega) = \frac{-\pi i\omega\ell}{\lambda_L^2 v_F}[\sigma_1(\omega) - i\sigma_2(\omega)], \tag{18}$$

where the complex conductivity $[\sigma_1(\omega) - i\sigma_2(\omega)]$ is given in Nam's paper.[6]

The surface impedance Z_s is calculated from the response function $\mathcal{K}(q,\omega)$ by the relation[26]

$$Z_s(\omega) = R_s(\omega) + iX_s(\omega) = 4i\omega \int_{-\infty}^{\infty} \frac{dq}{q^2 + \mathcal{K}(q,\omega)}. \tag{19}$$

Knowing the functional form of the response function $\mathcal{K}(q,\omega)$ in Eqs. (17) and (18) is not enough to determine $Z_s(\omega)$, since the set of fitting parameters listed in Table I as the "best fit" is not unique, and any other set with the same value of $\lambda_L(0)\sqrt{\xi_0/\ell}$ can also fit the surface-impedance data. In fact, the impedance data are only sensitive to $\lambda(0) = \lambda_L(0)\sqrt{\xi_0/\ell}$, so $\lambda_L(0)$, v_F, and ℓ are not separately determined. However, the penetration depth $\lambda(0)$ is determined uniquely from the surface impedance to be 3700 ± 300 Å.

Our data seems to be fit well by the weak-coupling model of surface resistance. The differences between R_s calculated in the weak-coupling model and that calculated using the strong-coupling limit have been investigated by Blaschke and Blocksdorf.[30] They show that, in the local and dirty limit, the differences are small enough that our measurements cannot differentiate between the results of the two models. It is also possible that the expressions for σ_1 and σ_2 given by Nam[6] reduce in the local and dirty limit to the same expressions derived by Mattis and Bardeen. This question of the local and dirty limit of Nam's theory will be further discussed by Chin.[31]

V. SUMMARY

We have demonstrated for the first time that surface-impedance measurements in stripline resonators and in microwave cavities agree when measuring films deposited under the same conditions. Determinations of R_s and the penetration depth λ are considered and have demonstrated excellent agreement.

The agreement between the cavity and stripline measurements has important implications for the characterization of the microwave properties of high-T_c materials. Many different films of the high-T_c materials have been evaluated by both stripline and cavity methods, and until now the sources of the observed discrepancies have not been understood. Based upon the measurements reported here, we can state that the discrepancies do not result from intrinsic differences between cavity and stripline methods.

We have further demonstrated good agreement between the measured temperature dependence of R_s and the $R_{\rm th}(\omega,T)$ calculated from the Mattis-Bardeen theory. The agreement leads us to conclude that the strong-coupling effect is not important in the local and dirty limit which NbN fulfills.

ACKNOWLEDGMENTS

The authors wish to thank Drs. R. Withers and J. Halbritter for a number of comments regarding the manuscript and Mr. W.T. Brogan for sample preparation. The research at MIT was supported in part by the Air Force Office of Scientific Research (AFOSR). The work at Rome Air Development Center was sponsored by the Department of the Air Force and was supported in part by the Laboratory Director's Fund. In addition G.D. was supported by the AFOSR University Research Residence Program. At MIT Lincoln Laboratory the work was supported in part by the Department of the Air Force and in part by the Defense Advanced Research Project's Agency through the Consortium for Superconducting Electronics.

APPENDIX: EFFECT OF THE FINITE SAMPLE THICKNESS

We have followed Sridhar's method[32] to calculate the effect of the finite sample thickness on the surface-impedance measurement using the stripline resonator. The effective surface impedance of a thin film of thickness t is[32]

$$Z_s(\omega,T,t) = \frac{8i\omega\pi}{t} \sum_{n=-\infty}^{\infty} \frac{1}{q_n^2 + \mathcal{K}(q_n,\omega,T)}, \tag{A1}$$

where q_n is the quantized wave vector associated with the standing-wave reflections at the surfaces defined by

$$q_n = \frac{2n\pi}{t}. \tag{A2}$$

The kernel $\mathcal{K}(q,\omega,T)$ is taken from Eq. (18) and gives

$$\begin{aligned} Z_s(\omega,T,t) &\approx 4i\omega\pi\lambda(0)\sqrt{\frac{\pi\Delta(0)}{\sigma_2\hbar\omega}} \coth\left(\frac{t}{2\lambda(0)}\sqrt{\frac{\hbar\omega\sigma_2}{\pi\Delta(0)}}\right) \\ &= Z_s(\omega,T,\infty)\coth\left(\frac{t}{2\lambda(0)}\sqrt{\frac{\hbar\omega\sigma_2}{\pi\Delta(0)}}\right). \end{aligned} \tag{A3}$$

In the limit $\hbar\omega \ll 2\Delta$ and $T \ll T_c$,

$$\begin{aligned} \sigma_1 &\approx 0, \\ \sigma_2 &\approx \frac{\pi\Delta(T)}{\hbar\omega} \end{aligned} \tag{A4}$$

and the penetration depth is given by[26]

$$\lambda(T) = \frac{2}{\pi}\lim_{\omega\to 0} \mathrm{Re}\int_0^{\infty} \frac{dq}{q^2 + \mathcal{K}(q,\omega)} \approx \lambda(0)\left(\frac{\hbar\omega\sigma_2}{\pi\Delta(0)}\right)^{-\frac{1}{2}}, \tag{A5}$$

so substitution of Eq. (A5) into Eq. (A3) gives

$$Z_s(\omega,T,t) \approx Z_s(\omega,T,\infty)\coth\left(\frac{t}{2\lambda(T)}\right). \tag{A6}$$

The correction given by Eq. (A6) was used in analysis of the stripline data.

[1]S. Isagawa, J. Appl. Phys. **52**, 921 (1981).
[2]D.C. Mattis and J. Bardeen, Phys. Rev. **111**, 412 (1958).
[3]J.P. Turneaure, Ph.D. thesis, Stanford University, 1967 (unpublished).
[4]J. Halbritter, Z. Phys. **266**, 209 (1974).
[5]S.B. Nam, Ph.D. thesis, University of Illinois, 1966 (unpublished).
[6]S.B. Nam, Phys. Rev. **156**, 470 (1967); **156**, 487 (1967).
[7]J. Geerk, U. Schneider, W. Bangert, H. Rietschel, F. Gompf, M. Gurvitch, J. Remeika, and J. M. Rowell, Physica B **135**, 187 (1985).
[8]K. E. Kihlstrom, R.W. Simon, and S.A. Wolf, Physica B **135**, 198 (1985).
[9]K. Mbaye, M. Pham Tu, N.T. Viet, L. Wartski, and J.C. Villegier, Rev. Phys. Appl. (France) **20**, 457 (1985); M. Pham Tu, K. Mbaye, L. Wartski, and J. Halbritter, J. Appl. Phys. **63**, 4586 (1988).
[10]J.Y. Juang, Ph.D. thesis, MIT, 1989 (unpublished); J.Y. Juang. D.A. Rudman, J. Talvacchio, and R.B. van Dover, Phys. Rev. B **38**, 2354 (1988).
[11]J. Talvacchio, J.R. Gavaler, and A.I. Braginski, *Metallic Multi-layers and Epitaxy*, edited by M. Hony, S. Wolf, and D.C. Gubser (Metallurgical Society, Wanendale, PA, 1988), p. 109; see also D.A. Rudman, J.Y. Juang, R.B. van Dover, S. Nakahara, D.W. Capone II, and J. Talvacchio, IEEE Trans. Magn. **MAG-23**, 831 (1987).
[12]A.C. Anderson, D.J. Lichtenwalner, and W.T. Brogan, IEEE Trans. Magn. **MAG-25**, 2084 (1989).
[13]M.S. DiIorio, A.C. Anderson, and B-Y. Tsaur, Phys. Rev. B **38**, 7019 (1988).
[14]D.E. Oates, A.C. Anderson, and P.M. Mankiewich, J. Superconduct. **3**, 251 (1990).
[15]A.J. Giles, S.K. Jones, D.G. Blair, and M.J. Buckingham, *Proceedings of the 43rd Annual Symposium on Frequency Control* (IEEE, New York, 1989), p. 89.
[16]H.A. Wheeler, Proc. IRE **30**, 412 (1942).
[17]H.A. Wheeler, IEEE Trans. Microwave Theory Tech. **MTT-26**, 866 (1978).
[18]J.D. Jackson, *Classical Electrodynamics*, 2nd ed. (Wiley, New York, 1975), Chap. 8.
[19]D.M. Sheen, S.M. Ali, D.E. Oates, R.S. Withers, and J.A. Kong (unpublished).
[20]T. Van Duzer and C.W. Turner, *Principles of Superconductive Devices and Circuits* (Elsevier, New York, 1981).
[21]M. Sucher and J. Fox, *Handbook of Microwave Measurements* (Polytechnic, New York, 1963), Vol. 2, Chap. 8.
[22]E.L. Ginzton, *Microwave Measurements* (McGraw-Hill, New York, 1957), Chap. 9.
[23]J.C. Slater, Rev. Mod. Phys. **18**, 441 (1946).
[24]R.E. Collin, *Foundations for Microwave Engineering* (McGraw-Hill, New York, 1966), p. 336.
[25]E. Maxwell, *Progress in Cryogenics* (Academic, New York, 1965), Vol. 5, p. 124.
[26]M. Tinkham, *Introduction to Superconductivity* (Krieger, Huntington, NY, 1980).
[27]T.P. Orlando, E.J. McNiff, Jr., S. Foner, and M. Beasley, Phys. Rev. B **19**, 4545 (1979).
[28]J. Halbritter (private communication).
[29]J. Halbritter, J. Less-Common Met. **139**, 133 (1988).
[30]R. Blaschke and R. Blocksdorf, Z. Phys. B **49**, 99 (1982).
[31]C.C. Chin (unpublished).
[32]S. Sridhar, J. Appl. Phys. **63**, 159 (1988).